ELSEVIER

Journal of Nuclear Materials 252 (1998) 156–161

journal of nuclear materials

Comment

Comments on "Behaviour of inert gas bubbles under chemical concentration gradients" by G.P. Tiwari

J.H. Evans [a,*], A. van Veen [b]

[a] *Department of Physics, Royal Holloway, University of London, Egham, Surrey TW20 0EW, UK*
[b] *Interfaculty Reactor Institute, Delft University of Technology, Mekelweg 15, 2629 JB Delft, The Netherlands*

Received 5 May 1997; accepted 22 October 1997

Abstract

The motion of inert gas bubbles induced by thermal vacancy gradients has previously been used by the present authors to understand gas bubble release in UO_2 and metals. This approach has been recently questioned by Tiwari. In the present letter, a critical discussion of his viewpoint is presented, together with an analysis of the important experimental results of Marachov et al. There appears to be good evidence for the disputed effect. © 1998 Elsevier Science B.V.

1. Introduction

In his recent paper [1], Tiwari discusses the behaviour of inert gas bubbles in vacancy gradients, with particular reference to a model [2–4] in which the movement of fission gas bubbles to grain boundaries in UO_2 during post-irradiation annealing is explained by the directed motion along the thermal vacancy gradient set up between the vacancy source at a boundary and the bubbles within a grain. A linear approach for the model, applicable to implanted inert gas bubble populations in metals, has also been published [5]. In this case the surface is the source of thermal vacancies. There appears to be agreement that a vacancy gradient exists under these circumstances but, using various arguments, Tiwari concludes that there is no evidence for bubble migration due to the gradient alone and thus that an additional temperature or stress gradient is necessary. The purpose of this letter is twofold: firstly it presents a critical discussion of the many points made by Tiwari, and secondly, since the results of Marachov et al. [6] seem to have been misinterpreted, these are presented again, together with a simulation of the bubble behaviour, including their movement under the vacancy gradient. A comparison of calculated and experimental results illustrates that the latter are indeed consistent with bubble movement, and thus contrary to Tiwari's conclusion.

As far as possible we shall follow the order of results as presented in Ref. [1]. One general point is worth mentioning at this stage. In order to be confident of a negative result regarding the movement of bubbles in vacancy gradients (particularly when there are clear theoretical arguments in favour of a positive result [5,7,8]), the results need to satisfy two criteria. The first is that from the data it must be absolutely clear that no bubble movement has taken place; the second is that we have to be certain that under the experimental circumstances being discussed, observable bubble movement should have been expected.

2. Discussion of Tiwari's arguments

2.1. His own experimental data

Tiwari begins by presenting evidence from his own work on the precipitation of helium bubbles in diffusion couples between Ni and irradiated Cu–B alloys. He concurs with previous experimental evidence for vacancy flow from thermal vacancy sources, but concludes that there is no evidence for bubble migration in the vacancy gradient

* Corresponding author. 27 Clevelands, Abingdon OX14 2EQ, UK. Tel.: +44-1235 525 059; fax: +44-1235 525 059.

PII S0022-3115(97)00327-9

set up during his experiment. However, no calculation is presented to show that bubble movement should have been large enough to be observed; thus it is impossible to draw any conclusion, negative or positive. This also applies to the work of van Gurp et al. [9] who used xenon bubble layers as markers in studying the formation of cobalt silicides during the annealing of evaporated cobalt on silicon.

To support his viewpoint in his own work, Tiwari adds that there is an absence of any preferential alignment of the bubble axes in the expected direction of movement. It is not clear where this idea comes from but it is well known that a bubble in equilibrium will always tend to a spherical shape in order to minimise its surface energy. Observations with transmission electron microscopy show, for example, that when two bubbles coalesce the spherical shape of the new bubble is re-established almost instantaneously, e.g. Refs. [10,11]. There is no justification, therefore, for using the presence of spherical shaped bubbles to infer a negative result on bubble migration.

2.2. Evans's model

In his next section, Tiwari discusses the model given by the present authors [5], introduces some of the comments of van Siclen [8], and, in his Fig. 4, presents the results of Marachov et al. [6]. In introducing the model, Tiwari admits that previous application to results on copper, nickel and silicon (also beryllium) do "indeed provide an indirect or circumstantial support" for the gas release behaviour in these systems, but he goes on to suggest that the results might equally be explained by the annealing of radiation damage and the break up of inert gas–vacancy complexes. This view ignores the fact that, in all the experimental cases, percentage values of inert gas concentrations were involved. In such cases, transmission electron microscopy (TEM) has demonstrated that the precipitation of the ion implanted inert gas in small bubbles must be expected during implantation [12]. Where TEM was applied in the metal cases quoted above, this result was confirmed. The possible break-up of small inert gas/vacancy complexes during high temperature annealing cannot possibly play any significant role in such a system.

Tiwari goes on to discuss the results of Marachov et al. [6] but much of this discussion seems based on misinterpretation. There is not space to discuss every point but in his comments on the presence of bubbles in the near surface regions, Tiwari appears not to have recognised that the initial deposition of helium is in a relatively thin layer at close to one micron from the implant surface (see Fig. 1, Ref. [6]), and, at the dose used (1×10^{17} He/cm^2), will almost certainly be present as sub-microscopic bubbles. Discussion of incubation time for bubble formation is therefore not appropriate and certainly there are no grain boundaries present as he claims (the 'artefacts' are photographic rather than structural). He gives the strong impression that, if bubble movement has taken place in the vacancy gradient, bubble movement out of the surface would have been expected. However, as we discuss in Section 3, this is not so. Possibly there has been confusion on the question of scale since Tiwari's scale marker on the reproduced Marachov et al. figure should read approximately 400 nm rather than his 2 nm. In his figure caption in the same figure, he is only correct in stating that the highest density of bubbles coincides with the region having the highest helium concentration if he concedes that the helium bubble profile has moved from its original peak at near 1 μm.

The suggestion by Tiwari that the results of Marachov et al. [6] and Evans et al. [13], might have been affected by beam heating is unfortunate. In both experiments, where systematic bubble effects were seen, out of microscope heating at, respectively, 1023 and 1650 K were required. Any effects from beam heating would have easily been recognised in unannealed material. In both studies the samples were subjected to conventional TEM and thus can hardly be compared with the work of Barnes and Mazey [10] cited by Tiwari, in which thin foils of copper were held on grids and then subjected to electron heating by removing condenser apertures.

The outline of the model as given by Tiwari, see also his fig. 5, is generally accurate, but it is difficult to understand his main objection, based on the assertion that "quilibrated bubbles will not accept vacancies because they have already achieved equilibrium". While the total number of vacancies in an equilibrium bubble may stay constant, the dynamic nature of vacancy evaporation and absorption in such a bubble has been known since the classic work of Greenwood et al. [14] and is crucial in the present context. Van Siclen presents the simplified picture that "bubbles move since the vacancy absorption at the bubble is proportional to the vacancy concentration there (and so is anisotropic) while vacancy emission is isotropic". Although easily visualised, this is not quite accurate; as outlined in more detail in Refs. [5,7], the vacancy fluxes are proportional to the radial gradient of the vacancy concentration at the bubble surface. Nevertheless, there can be no doubt that, theoretically, bubble movement is to be expected in a vacancy gradient. Tiwari's objection to the theory is unfounded.

2.3. Results of Pati and Barrand

In his Section 4, Tiwari discusses the results of Pati and Barrand [15] who examined helium gas bubble formation in an irradiated Cu–B alloy, and again concludes that the experimental results provide no evidence for bubble migration induced by the vacancy flux. However, there is no guide to how such migration would have manifested itself nor how much migration might have been expected. It is thus not at all clear how Tiwari reaches his negative conclusion. The discussion on the morphology of bubbles

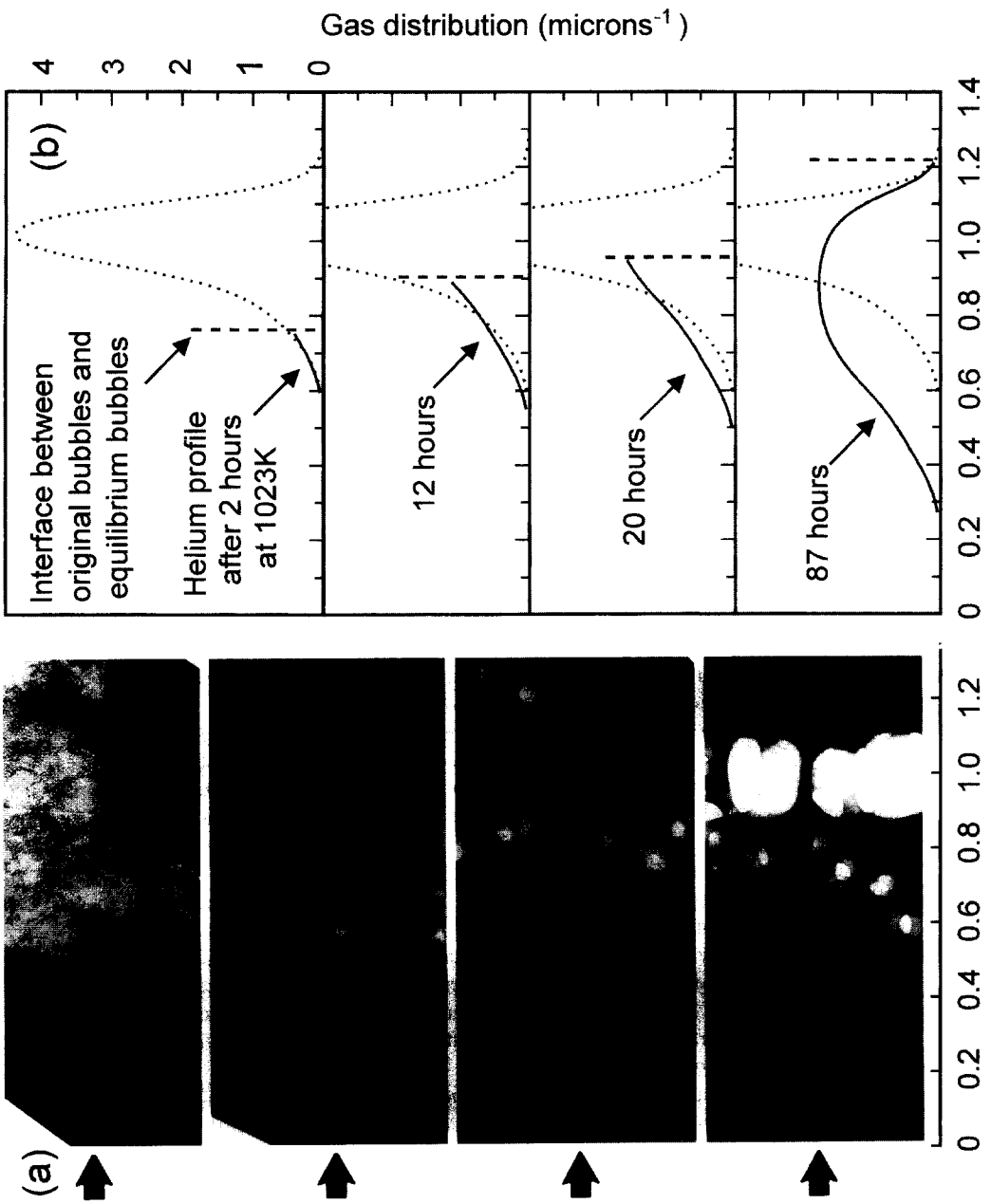

Fig. 1. (a) The cross-sectional electron microscope data of Marachov et al. [6] showing the evolution, following a 500 keV implant at 293 K, of helium bubbles in four nickel samples annealed at 1023 K to different times, top to bottom, 2, 12, 20 and 100 h. Arrows show implant direction. (b) Results of the model in text showing the movement of gas atom profiles during annealing. These can be directly compared with the four micrographs in (a).

does not immediately seem relevant (the morphology even in the same sample, figs. 6 and 7 appear very different) while the quoted absence of any sharp step between large and small bubbles must depend on several factors such as the original distribution of helium and the time at which the micrographs were taken relative to the complete anneal.

Tiwari's other approach is to compare the Pati–Barrand micrographs, his figs. 6 and 7, with the rate equation

$$dS/dt = D_v \Omega C_{sv}/x_i \quad (1)$$

in order to explain the bubble distributions observed. This equation, where D_v is the vacancy diffusivity, Ω is the atomic volume of the metal, and C_{sv} is the vacancy concentration at the surface, gives the instantaneous swelling rate at a depth x_i where the incoming vacancies have created an interface between equilibrated (coarsened) bubbles and the original bubble population. (See Tiwari, fig. 5 and Evans and van Veen [5], fig. 1 for further details.)

Eq. (1) is correct, but Tiwari's conclusion that it predicts a swelling that varies inversely with distance from the surface is in error. The reason for this is that x_i is time dependent and thus, in the present context, it is impossible for the equation to give any guidance to the final distribution of swelling with depth from the surface. In calculating this distribution, the value of (dx_i/dt) has to be considered. As given in the equations set out in Ref. [5], this value depends on the vacancies needed to bring the bubbles at x_i to equilibrium. For the particular case where bubble movement is ignored and equilibrium bubbles have all the same size, then the final variation of swelling with depth will exactly follow the original gas distribution.

3. Modelling of the Marachov et al. results

3.1. Background

Marachov et al. [6] used cross-sectional TEM to follow the annealing of helium bubbles introduced into nickel using 500 keV helium ions. The results were important in directly demonstrating the initial development of bubble coarsening in regions nearest the surface (see Fig. 1). In agreement with Barnes et al. [16,17], the results thus showed that during annealing the surface was the dominant source of thermal vacancies. As a consequence of the resulting vacancy flux, Evans [2] pointed out that a vacancy gradient had to exist between the surface and the bubbles which had previously nucleated in the narrow helium implanted peak, and that this gradient had the ability to induce bubble movement up the gradient. Although rough calculations by Evans [2] and Van Siclen [8] suggested that the results of long time annealing in the Marachov results were consistent with some bubble movement towards the surface, the renewed interest in this topic in Tiwari's paper makes it worthwhile to examine the bubble behaviour in more detail.

3.2. Description of modelling

We apply the approach described by Evans and van Veen [5] to calculate the expected development of the bubble profiles in the Marachov et al. [6] results. Essentially the methodology divides the material depth and the gas atom profile into slices allowing computer simulation to follow, first, the movement of the interface between the coarsened equilibrium bubbles and the original small bubbles, and second, the subsequent movement of the gas population in response to the vacancy gradient and annealing parameters. As discussed in Ref. [5], the expression for the net movement of bubbles relative to the surface followed that of Geguzin and Krivoglas [7] as

$$V_b = -2D_v dC_v/dx, \quad (2)$$

where dC_v/dx is the vacancy gradient. This equation was also derived by electrostatic analogy and is in the range given by van Siclen [8]. It is the fortunate absence of the bubble size in this equation that allows the calculation to disregard the bubbles as such. Effectively the bubbles are smeared out and incorporated into the gas atom profile, allowing changes in the profile to be followed. In the modelling, D_v and C_v are incorporated into the self-diffusion coefficient, D_{sd}.

For these calculations, the initial helium profile for 500 keV helium ions in nickel was calculated with TRIM90 [18]. The peak gas concentration was at a depth of 1.015 μm, very close to the 1.0 μm value given by Marachov et al. [6] (see fig. 1 in their paper), although they had assumed a Gaussian distribution. As is clear from both linear and grain modelling [4,5], the accumulation of vacancies in growing equilibrium bubbles to their final size (the number of vacancies required per gas atom) is a crucial factor in controlling all the qualitative aspects of bubble movements particularly the final gas profile at the end of the anneal. This vacancy accumulation has been defined in previous papers as ΔS and is identical to the local fractional swelling of the equilibrium bubbles (before any induced bubble movement might have reduced this swelling), i.e. $\Delta S = G/(\rho_g \Omega)$, where G is the gas concentration fraction, ρ_g the gas packing density in bubbles and Ω is the atomic volume of the matrix material.

Some judgement is needed in respect to the equation of state to evaluate ρ_g, but for the application that follows ($T = 1023$ K, bubble size, 32.5 nm), the van der Waals equation is appropriate. Using the equilibrium bubble equation, $p = 2\gamma/r$, where γ is the surface energy and r is the bubble radius, and replacing G/Ω by $f(x)\phi$, where $f(x)$ is the normalised gas distribution profile and the helium implant dose, we derive the equation

$$\Delta S = f(x)\phi[23.7 + 4.16 \times 10^{-3} rT/\gamma]/6.03 \times 10^6, \quad (3)$$

where the units of $f(x)$, ϕ, r and γ are, respectively, (cm^{-1}), (10^{17} He atoms/cm^2), (nm) and (J/m^2). In the present case, $f(x)$ was calculated from the initial TRIM helium distribution while the other parameters used were $T = 1023$ K, $\gamma = 1.8$ J/m^2 (nickel [20,21]), and $r = 32.5$ nm (from the micrograph of Marachov et al. [6], see below). The dynamics of the annealing process was controlled by the nickel self-diffusion coefficient. At 1023 K, a value of 5.21×10^{-15} cm^2/s [8,22] was used.

3.3. Results

The results of this approach are given in Fig. 1b and can be compared with the experimental results from fig. 2 of Marachov et al. [6] which are reproduced here in Fig. 1a and show the evolution of the bubble populations with annealing time. Marachov et al. gave no scale marker in their figure, but it is reasonable to assume that the large bubbles in their final 100 h micrograph are centred close to the original helium peak near 1 μm. Thus, both Fig. 1a and b here have the same depth scale. While the early times can be directly compared, the computed results show that as far as any bubble movement was concerned, the annealing was over at 87 h as the interface between the equilibrium and original bubbles reached the end of the helium profile. Thus, although further bubble coalescence may have taken place, as far as the helium gas distribution is concerned, this last calculation is equivalent to the experimental 100 h micrograph.

In the calculations it is clear that the bubble movement up the vacancy gradient induces a marked change in the helium gas profile during annealing. Although no gas is predicted to have left the sample surface, gas atoms originally on the periphery of the helium profile at a depth of 0.6 μm are calculated to have moved over 300 nm, while the helium peak at near 1 μm has changed to a much broader profile with a flat maximum near 0.85 μm. A direct visual comparison between this calculated data and the four experimental micrographs certainly suggests good agreement in the bubble evolution sequence, particularly the limited change in the 2 h anneal, the movement of the equilibrium bubble/original bubble interface seen experimentally in the 12 and 20 h anneals, the large difference between the 20 and 100 h anneals in the depth around 0.7 μm, and the final distribution of bubbles centred at the same depth. It should be emphasised that in the calculations, all the parameters are reasonably well known. The greatest uncertainty probably lies in the chosen self-diffusion coefficient though it is reassuring that at 1023 K the careful assessment of Seeger and Mehrer [23] give a value of 4×10^{-15} cm^2/s, only a little smaller than the value used. In any case the value of D_{sd} does not affect the final profile at the end of the anneal, only the rate at which it is approached.

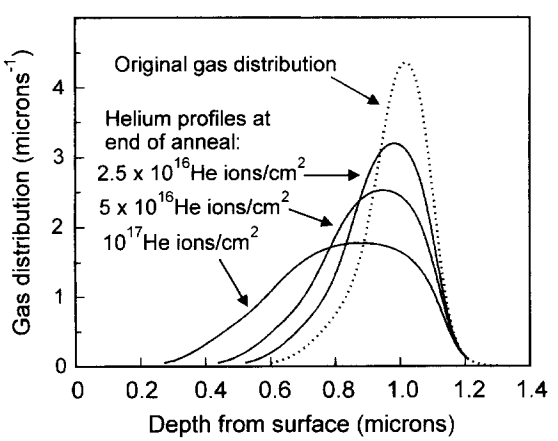

Fig. 2. Calculated end-of-anneal gas atom profiles showing the effect of gas level on induced profile (bubble) movement. For a dose of 1×10^{16} He ions/cm^2 (not shown) the final profile was close to that of the original gas distribution.

The comparison between the calculated and experimental results can be discussed further for the depth range 0.6 to 0.8 μm. The calculations show that by combining the value of helium implant dose with the average value of normalised gas distribution curves for the start and finish of the anneal sequence, the average helium concentration in this range has changed almost fivefold during the anneal from 3.05×10^{20} to 1.47×10^{21} helium atoms/cm^3. The question is whether this final predicted helium level is reflected in the bubble distribution seen experimentally.

This question has been addressed by examining in detail the experimental data given by Marachov et al. (Fig. 1a in the present paper). For the 100 h anneal, the bubble parameters have been carefully measured over the 0.6–0.8 μm depth range. The area in question, 200×602 nm^2, contains 21 bubbles with a root mean cube average size of 32.5 nm. The size here is the edge length since all the bubbles appear to have cube symmetry although there is some truncation analogous to that observed by Niwase et al. [24] for similar helium bubbles in nickel annealed over the 923–1048 K range. Although the computer calculations as described tacitly assume spherical bubbles, they are independent of the change to a cube morphology; this follows since the equilibrium pressure in a cubic bubble with a $2r$ edge length is identical with that in a spherical bubble of diameter $2r$ [25].

In order to proceed, we have taken the sample thickness as 175 nm, thus giving a bubble density of 1.0×10^{15}/cm^3. Taking the equilibrium bubble pressure ($\gamma = 1.8$ J/m^2) for the average size, together with the van der Waals gas law and the cubic bubble shape, leads in turn to the helium packing density in bubbles, to the average number of helium atoms per bubble and finally, together with the bubble concentration, to the local helium concentration. In this way, the value of 1.65×10^{21} He atoms/cm^3 was obtained for the average helium concentration lying in the 0.6–0.8 μm depth range after the final anneal at 1023 K.

Given that this helium level will be reduced proportionately by the degree of truncation in the bubble shape, the agreement with the predicted value of near 1.5×10^{21} helium atoms/cm^3 is very satisfying. Although small errors in the values of surface energy and sample thickness are possible, it is hard to escape the conclusion that by the end of the anneal sequence, the Marachov et al. [6] results give clear evidence of bubble movement. This contradicts Tiwari's suggestion that there is no evidence for bubble movement under a thermal vacancy gradient.

3.4. Effect of helium level on bubble movement

Although we believe that in the Marachov data, bubble movement has induced a significant change in gas atom profile with depth, it is important not to assume that such bubble movement must always be present. The level of gas plays a vital role. If levels are low and bubbles small, then relatively few vacancies are needed to bring bubbles to equilibrium. Thermal equilibrium is then set up rapidly over the volumes containing bubbles, thus strongly limiting the time over which the vacancy gradient can exist to induce bubble migration. In the Marachov et al. experiment (dose 10^{17} He ions/cm^2), the helium level at the peak of the profile was nearly 5%. To illustrate the effect of reducing the gas level, computer calculations have also been made for lower doses but maintaining other parameters as before. In Fig. 2, the results for the three doses, 1×10^{17}, 5×10^{16} and 2.5×10^{16} He ions/cm^2, annealed to completion are compared. The decrease in the profile movement with drop in gas concentration is very evident. For a dose of 1×10^{16} ions/cm^2, the profile was hardly changed from the as-implanted profile.

It is not possible to make any rule about detecting gas bubble movement in vacancy gradients. As demonstrated above, low gas levels mitigate against movement but as shown in Eq. (3), an increase in the equilibrium bubble radius could provide some compensation. The optimum method of detecting a bubble movement might well be in a gas release experiment where the original gas levels were up to the surface, allowing any induced bubble movement to be immediately reflected in gas release.

Returning to the experimental data given in Tiwari's paper, the preceding discussion highlights the general point that only by examining bubble radii, gas concentration levels and gas profiles can any firm deductions be made on ascertaining whether experiments should be expected to show bubble movement.

4. Conclusions

In his conclusion Tiwari states "that the mere presence of a vacancy flux originating from a surface or interdiffusion does not seem to be enough to induce migration of inert gas bubbles". This is of course correct: it is easy to show, as in Section 3.4, that situations will exist where effects are minimal. However, this can hardly be a rational basis for concluding, as Tiwari has done, that an additional driving force such as stress or a temperature gradient appears to be necessary. We would contend with our discussions in the present letter, that Tiwari has nowhere presented any evidence to support this. In contrast, our computed results appear to give an accurate simulation of the Marachov et al. data suggesting that bubble movement under a vacancy gradient does take place as expected theoretically. This must help to validate the models of high temperature gas release for irradiated UO_2 [2–4] and metals [5] that are based on this bubble movement.

References

[1] G.P. Tiwari, J. Nucl. Mater. 232 (1996) 119.
[2] J.H. Evans, J. Nucl. Mater. 210 (1994) 21.
[3] J.H. Evans, J. Nucl. Mater. 225 (1995) 302.
[4] J.H. Evans, J. Nucl. Mater. 238 (1996) 175.
[5] J.H. Evans, A. van Veen, J. Nucl. Mater. 233–237 (1996) 1179.
[6] N. Marachov, L.J. Perryman, P.J. Goodhew, J. Nucl. Mater. 149 (1987) 296.
[7] Ya.E. Geguzin, M.A. Krivoglas, Migration of Macroscopic Inclusions in Solids, Consultants Bureau, New York, 1973.
[8] C.DeW. Van Siclen, Philos. Mag. Lett. 72 (1995) 41.
[9] G.J. van Gurp, W.F. van der Weg, D. Sigurd, J. Appl. Phys. 49 (1978) 4011.
[10] R.S. Barnes, D.J. Mazey, Proc. R. Soc. A 275 (1963) 47.
[11] P.B. Johnson, D.J. Mazey, Radiat. Eff. 53 (1980) 195.
[12] S.E. Donnelly, J.H. Evans (Eds.), Fundamental Aspects of Inert Gases in Solids, Plenum, New York, 1991.
[13] J.H. Evans, A. van Veen, K.T. Westerduin, J. Nucl. Mater. 195 (1992) 21.
[14] G.W. Greenwood, A.J.E. Foreman, D.E. Rimmer, J. Nucl. Mater. 1 (1959) 305.
[15] S.R. Pati, P. Barrand, J. Nucl. Mater. 31 (1969) 117.
[16] R.S. Barnes, G.B. Redding, A.H. Cottrell, Philos. Mag. 3 (1958) 97.
[17] R.S. Barnes, Philos. Mag. 5 (1960) 635.
[18] J. Biersack, L.G. Haggmark, Nucl. Instrum. Meth. 174 (1980) 257.
[20] P.S. Maiya, J.M. Blakely, J. Appl. Phys. 38 (1967) 698.
[21] V.K. Kumikov, Kh.B. Khokonov, J. Appl. Phys. 54 (1983) 1346.
[22] D.R. Lide (Ed.), CRC Handbook of Chemistry and Physics, 73rd ed., CRC, Boca Raton, FL, 1992, pp. 12–136.
[23] A. Seeger, H. Mehrer, in: A. Seeger, D. Schumacher, W. Schilling, J. Diehl (Eds.), Proc. Int. Conf. on Vacancies and Interstitials in Metals, Jülich 1968, North-Holland, Amsterdam, 1970, p. 1.
[24] K. Niwase, T. Ezawa, F.E. Fujita, H. Kusanagi, H. Takaku, Radiat. Eff. 106 (1988) 65.
[25] P.J. Goodhew, Metal Sci. 15 (1981) 377.